# Annexin A2 is required for the early steps of cytokinesis

Christelle Benaud[1,2,*], Gaëlle Le Dez[1,2], Svetlana Mironov[1,2], Federico Galli[1,2], David Reboutier[1,2] & Claude Prigent[1,2]

## Abstract

Cytokinesis requires the formation of an actomyosin contractile ring between the two sets of sister chromatids. Annexin A2 is a calcium- and phospholipid-binding protein implicated in cortical actin remodeling. We report that annexin A2 accumulates at the equatorial cortex at the onset of cytokinesis and depletion of annexin A2 results in cytokinetic failure, due to a defective cleavage furrow assembly. In the absence of annexin A2, the small GTPase RhoA—which regulates cortical cytoskeletal rearrangement—fails to form a compact ring at the equatorial plane. Furthermore, annexin A2 is required for cortical localization of the RhoGEF Ect2 and to maintain the association between the equatorial cortex and the central spindle. Our results demonstrate that annexin A2 is necessary in the early phase of cytokinesis. We propose that annexin A2 participates in central spindle–equatorial plasma membrane communication.

## Introduction

During cytokinesis, the coupled remodeling of the plasma membrane, the actomyosin cortex and the microtubule spindle drive the ingression of the cleavage furrow between the two sets of separated sister chromatids [1]. Assembly and contraction of the actomyosin ring at the plane of division involve the recruitment of scaffolding proteins, actin polymerization and myosin activation. Regulatory and structural elements of the contractile ring start to organize in very early anaphase as chromosomes begin to separate. They progressively concentrate to become restricted to the equatorial plane as the cell progresses through anaphase. The cortical reorganization is triggered by the small GTPase RhoA that directly activates several proteins that control the dynamics of the actin cytoskeleton leading to the formation of the contractile ring and its

contraction. It promotes filamentous actin polymerization [2] and activation of the ROCK signaling cascade leading to activation of myosin II, which assembles and contracts the actomyosin ring [3]. One key regulatory step of cytokinesis is thus the spatio-temporal activation of RhoA at the equatorial cortex. The MKLP1–MgcRacGAP centralspindlin complex accumulation at the midpoint of the central spindle is believed to provide the spatial clue that directs the equatorial activation of RhoA. The MgcRacGAP moiety of the complex directs the recruitment of the Rho guanidine exchange factor (GEF) Ect2 to the central spindle, where it has been proposed to locally activate cortical RhoA, since depletion of MKLP1, MgcRacGAP and Ect2 all result in the loss of spatial regulation of RhoA [4–6]. However, the mechanism of communication between the spindle and the equatorial cortex remains to be clarified. Where and how RhoA is regulated remains a central question to understand the early steps of cytokinesis. The possibility of a synergy between several mechanisms cooperating to restrict the localization and activation at the equatorial cortex needs to be explored.

Annexin A2 is a member of the annexin family of small calcium-binding proteins that displays high affinity for anionic phospholipids and preferentially associates with membranes enriched in phosphatidylinositols (PIPs). In addition, annexin A2 is an actin-binding protein, which is recruited to the site of actin assembly at cellular membranes [7,8], both on the cytoplasmic side of vesicles [9–11] and on the inner side of the plasma membrane [12]. Annexin A2 is involved in the establishment of epithelial cell polarization via the recruitment of various members of the Rho family of small GTPases regulating the actin cytoskeleton [13]. Annexin A2 is also required for RhoA recruitment during polarized cell mobility [14] or during growth factor-involved morphological changes [15].

Even though no role of annexin A2 during mitosis has yet been reported, annexin A2 has been identified in the proteome and phosphoproteome of the mitotic spindle [16]. Its link to dynamic membrane-associated actin cytoskeleton remodeling during various cellular processes has prompted us to examine the implication of annexin A2 during cytokinesis. In this work, we show that depletion of annexin A2 by RNAi results in cytokinetic failure. Cellular analysis reveals that annexin A2 accumulates at the cytokinetic furrow

1   Centre National de la Recherche Scientifique, UMR 6290, Equipe Labellisée Ligue 2014, Rennes, France
2   Institut de Génétique et Développement de Rennes, Université de Rennes I, Rennes, France
    *Corresponding author. Tel: +33 2 23 23 45 94; E-mail: christelle.benaud@univ-rennes1.fr

and its downregulation prevents or severely compromises the accumulation of the cortical ring components at the equator. We further show that annexin A2 depletion impairs the polarized RhoA accumulation at the equatorial cortex. While Ect2 and the centralspindlin components are correctly recruited to the midzone, no Ect2 is detected at the plasma membrane and the anchorage of the central spindle to the plasma membrane is lost. Our data thus indicate that annexin A2 is required for the early steps of cytokinesis to set up the RhoA signaling pathway at the cortical ring.

## Results and Discussion

### siRNA-mediated downregulation of annexin A2 results in the formation of binucleated cells

To investigate the function of annexin A2 during mitosis, HeLa cells were treated with four independent siRNAs directed against annexin A2. Two of the siRNAs resulted in the downregulation of the protein, Anx2-1 siRNA being more efficient than Anx2-8, whereas Anx2-2 and Anx2-4 siRNAs and the control siRNA did not alter the cellular level of the protein (Fig 1A). Anx2-1 siRNA will be used from here on, unless otherwise specified. The presence of binucleated cells was detectable 48 h post-siRNA transfection of an asynchronous cell population and was directly proportional to the efficiency of annexin A2 depletion, since more binucleated cells were detectable in the population treated with Anx2-1 than Anx2-8 siRNA (Fig 1B and D: 64% versus 24% of the filmed dividing cells, $n \geq 129$). Similar results were obtained in U2OS cells (Supplementary Fig S1).

### Decrease in levels of annexin A2 leads to early cytokinetic failure

To characterize the defect leading to the binucleated cell phenotype, we performed live cell imaging of annexin A2-depleted cells (Fig 1C). In control siRNA-treated cells, full cleavage furrow ingression was detected within 9 min and cytokinetic bridge formation 15 min following anaphase onset. Cells depleted for annexin A2 displayed the same dynamics of chromosome segregation as the control cells; however, 64% of the cells transfected with Anx2-1 siRNA and 24% of the cells transfected with Anx2-8 siRNA were unable to complete furrow ingression and to form a cytokinetic bridge. While a population of cells displayed no clear cleavage

furrow formation, nor ingression (37%), others displayed partial furrow ingression either on both sides (11%) or only on a single side of the cells (15%), followed in all cases by regression and formation of a binucleated cell (Fig 1D Anx2-1 and Supplementary Movies S1, S2, S3 and S4). The variability in the extent of the phenotype observed is most likely reflecting the level of annexin A2 depletion. Time-lapse microscopy thus reveals a defect in the early steps of cytokinesis. To ensure that this cytokinetic defect was specific to the downregulation of annexin A2, we generated HeLa cells stably expressing Anx2-1 siRNA-resistant annexin A2 fused with the GFP tag at its C-terminal end, which has been reported not to affect annexin A2 cellular localization [11] (Supplementary Fig S2A). Expression of siRNA-resistant annexin A2 indeed substantially suppressed the cytokinetic defect induced by annexin A2 depletion (66% rescue, $n \geq 100$) (Fig 1E).

Time-lapse imaging of annexin A2-GFP using spinning-disc confocal microscopy to examine live annexin A2 localization during cytokinesis indicates that albeit annexin A2 is present at the plasma membrane in metaphase, it strongly accumulates at the equatorial membrane at the site of the cytokinetic furrow during anaphase (Fig 1F and Supplementary Movie S5). The accumulation of annexin A2 occurs at the onset of furrow constriction. Some vesicular staining in between the two sets of chromosome and in close proximity of the equatorial membrane can also be observed. Quantification of fluorescent intensity of annexin A2-GFP in early cytokinesis (Fig 1F) both at the polar and at the equatorial membrane (as described in Fig 3D) indicates a ratio of fluorescence equator to pole of 3.3 (SD = 0.77, $n = 22$) confirming the accumulation of annexin A2 at the cytokinetic furrow.

### Downregulation of annexin A2 impairs actomyosin ring formation

To investigate the nature of the cytokinetic defect observed in annexin A2-depleted cells, we first evaluated their ability to form an actomyosin ring at the equatorial cortex. HeLa cells transfected with the control or Anx2 siRNA were synchronized at the G2/M transition with the RO 3306 CDK1 inhibitor and then released to reach anaphase. Both live cell imaging of actin dynamics (Fig 2A and Supplementary Movies S6 and S7) and immunofluorescence analysis (Fig 2B) revealed that annexin A2 is required for the formation of the filamentous actin ring at the equatorial cortex during anaphase. In cells lacking annexin A2, actin poorly accumulated at

---

**Figure 1.  Depletion of annexin A2 results in cytokinetic failure.**

A   Immunoblot analysis of total cell extracts of HeLa cells transfected with control RNAi or four independent Anx2 siRNAs (1, 2, 4, 8). Extracts were probed with anti-annexin A2 and anti-tubulin antibodies.

B   Bi-nucleation of asynchronous HeLa cells 48 h after transfection with the indicated siRNA.

C   Phase contrast live cell imaging of HeLa cells transfected with control siRNA or Anx2-1 siRNA. Time point $t = 0$ was set at the metaphase–anaphase transition.

D   Quantification of the cytokinetic phenotypes observed in live cell imaging after transfection with control siRNA, Anx2-1 siRNA or Anx2-8 siRNA ($n \geq 167$ dividing cells) $P = 0.001$ for three independent experiments, Student's $t$-test. The categories asymmetric furrow ingression, no/weak furrow ingression and partial furrow ingression and regression all resulted in the formation of binucleated cells. Phenotypes illustrated in Supplementary Movies S1, S2, S3 and S4.

E   Dividing HeLa and siRNA-resistant annexin A2-GFP HeLa cells were monitored by video microscopy 36 h post-transfection with control or Anx2-1 siRNA. Quantification of binucleation is presented in percentage of number of cells undergoing mitosis during the time lapse (graph). Error bars, SD of three experiments ($n \geq 100$). *$P = 0.005$, Student's $t$-test. Cells were fixed and labeled for tubulin, DNA and GFP (right panel). Immunoblot characterizing the cells is shown in Supplementary Fig S2.

F   Spinning confocal images of annexin A2-GFP HeLa cells (LUT fire). Time point $t = 0$ was set at the metaphase–anaphase transition. Scale bar, 10 μm. Eq/P represents the ratio of equatorial over polar GFP intensity as described in Fig 3D (SD = 0.77, $n = 22$). Full sequence presented in Supplementary Movie S5.
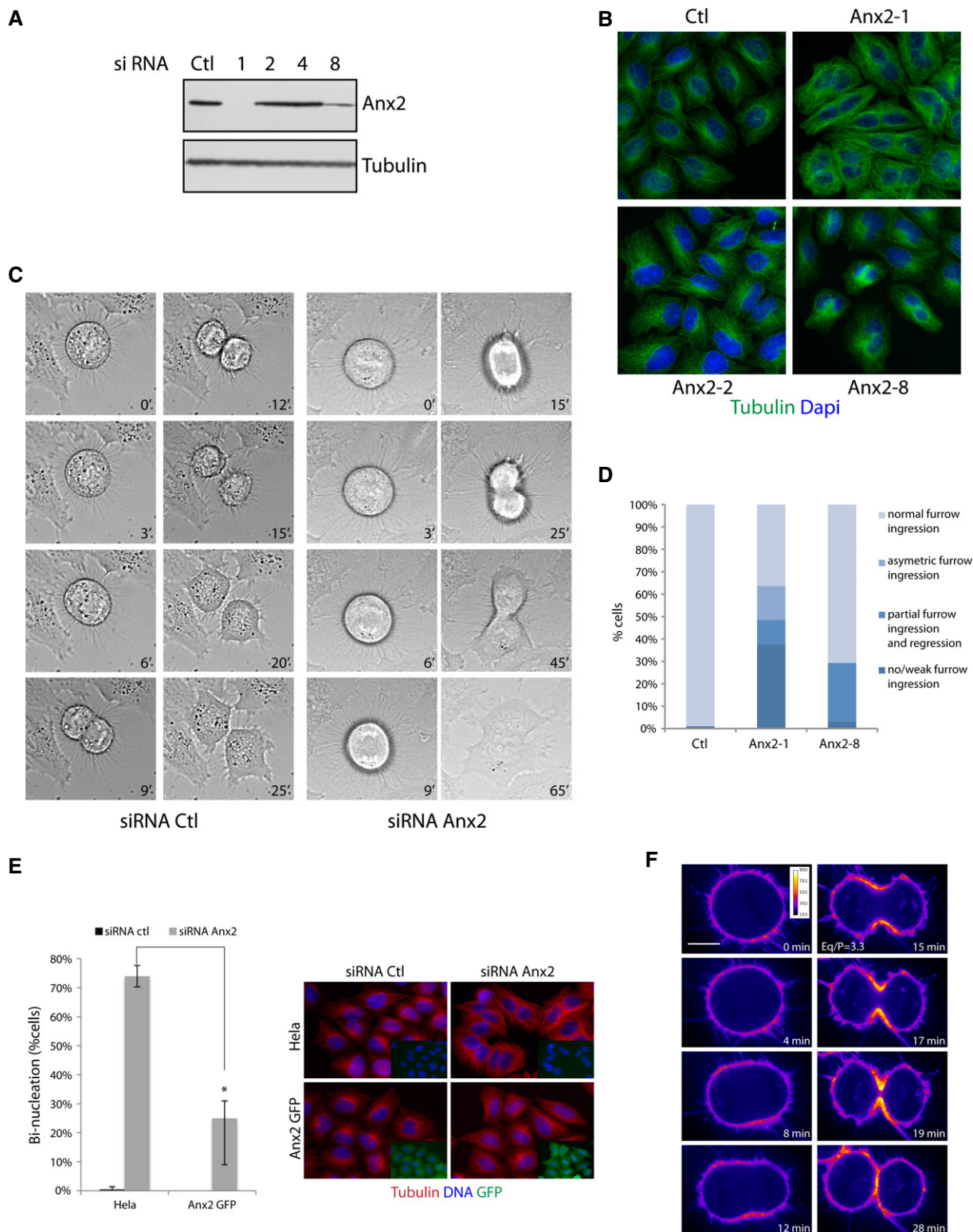
**A**



**B**



Tubulin Dapi

**C**



siRNA Ctl     siRNA Anx2

**D**



- normal furrow ingression
- asymetric furrow ingression
- partial furrow ingression and regression
- no/weak furrow ingression

**E**



- siRNA ctl
- siRNA Anx2

Tubulin DNA GFP

**F**



**Figure 1.**

the presumptive furrow or accumulated on a single side of the equatorial cortex (Fig 2B). Furthermore, in asymmetrically contracting cells, actin also distributed to the poles of the cell (Fig 2A and B). Similarly, downregulation of annexin A2 severely diminished the accumulation of myosin II at the cell equator observed in control cells (Fig 2C). We also examined the recruitment of the contractile ring scaffolding protein anillin, which concentrates at the cleavage furrow during cytokinesis (Fig 2D). Sixty-four percent of the cells
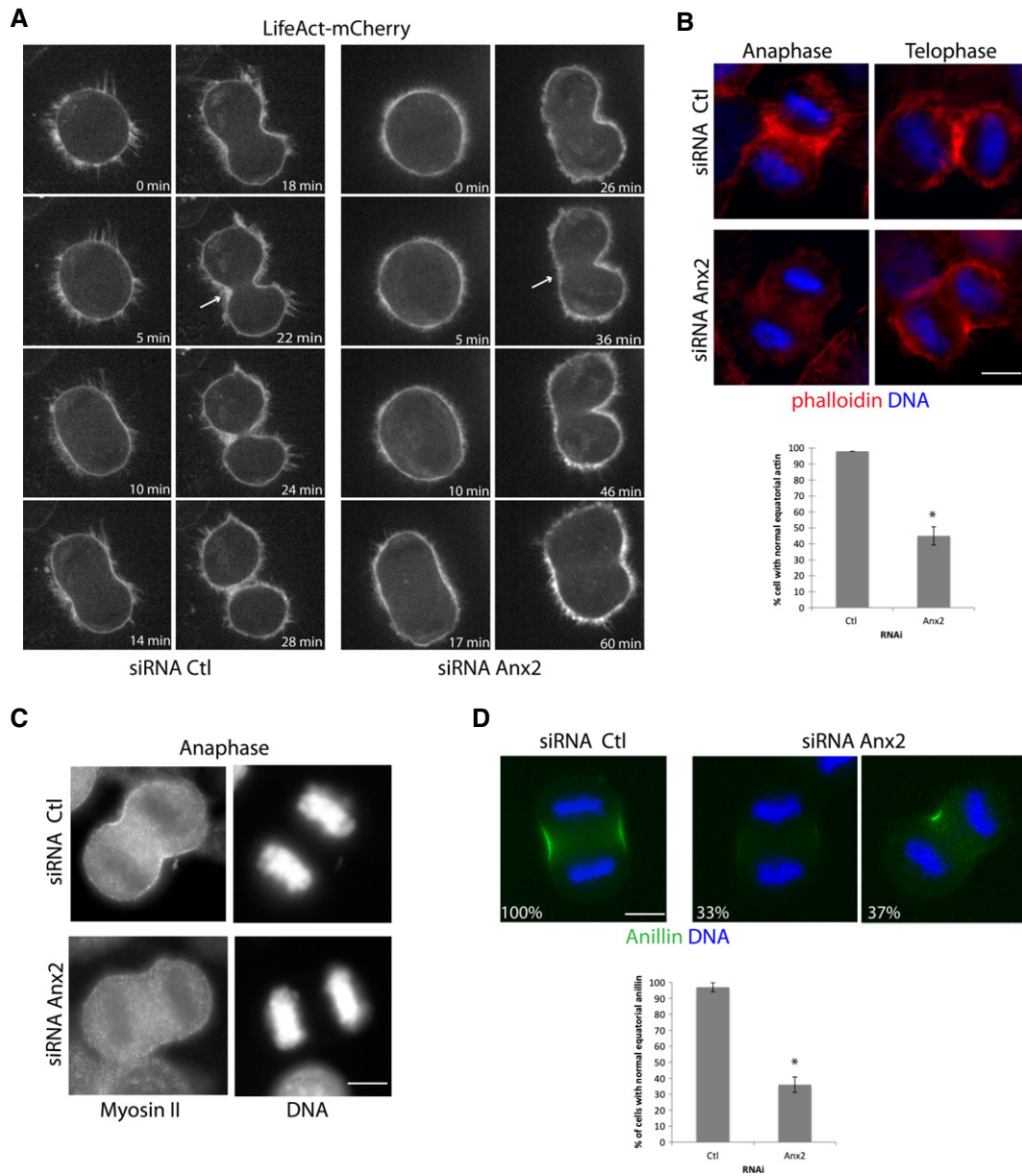
**Figure 2. Annexin A2 downregulation abrogates the actomyosin ring formation.**

A    Spinning confocal images of HeLa cells expressing the filamentous actin biosensor Life Act. Anx2 siRNA-transfected cells undergoing asymmetric furrow ingression display decreased actin accumulation on the non-invaginating side of the equatorial cortex (arrow) compared to the Ctl RNAi-treated cells. For full sequence, see Supplementary Movies S6 and S7.

B–D  HeLa cells treated with Ctl or Anx2 siRNA were synchronized at G2–M transition, released to reach anaphase and early telophase and then analyzed by immunofluorescence for contractile ring elements. Cells were analyzed for F-actin with phalloidin (B) and antibody against myosin II (C). Percentage of cells displaying normal equatorial actin staining following transfection with Ctl or Anx2 siRNA (B, graph). Error bars, SD of three experiments ($n \geq 100$). *$P = 0.001$, Student's $t$-test. Cells were analyzed for anillin (D). Percentages indicate the fraction of cells displaying the phenotype represented in the image among the cells scored in anaphase ($n = 80$). Quantification of the percentage of cells presenting normal equatorial anillin staining (D, graph). Error bars, SD of three experiments ($n \geq 60$ each). *$P = 0.001$, Student's $t$-test. Scale bars, 10 μm.

treated with annexin A2 siRNA displayed an abnormal localization of anillin, with either a reduced cortical recruitment (33%) or a recruitment on a single side of the cell equator (37%), which is consistent with the observed cleavage furrow phenotype of partial and asymmetric constriction, respectively. Our results thus indicate that decrease of annexin A2 severely compromised the formation of the filamentous actin ring and abrogated the accumulation of the contractile ring components anillin and myosin II at the equatorial cortex, thereby affecting the formation and ingression of the contractile ring at the equator during anaphase.

**Annexin A2 is required for proper RhoA localization**

The small GTPase RhoA pathway controls the assembly and contraction of the actomyosin cytokinetic ring through the activation of different effectors. Localized RhoA activation at the equatorial cortex regulates both actin polymerization and myosin recruitment and activation and is furthermore required for anillin localization [2,3,17]. The strong defect in contractile ring assembly in cells depleted for annexin A2 prompted us to investigate whether RhoA is recruited to the equatorial cortex and accumulated at the contractile furrow. Although the overall cellular level of RhoA was not decreased in cells depleted for annexin A2 (Fig 3B), the recruitment at the equatorial cortex was strongly decreased in 38% of cells or asymmetric in another 38% of cells ($n \geq 50$) (Fig 3A and Supplementary Fig S1D U2OS). Co-expression with Anx2 siRNA of HA-tagged siRNA-resistant annexin A2 (Supplementary Fig S2C) reversed the diminished RhoA equatorial localization (Fig 3E), but not the co-expression of the I7L8/EE annexin A2 mutant, which cannot form the $Anx_2S100A10_2$ heterodimer (Supplementary Fig S2B). To address whether this decrease was due to a lack of cortical recruitment, we generated a cell line stably expressing MyrPalm-GFP and used this GFP fluorescence to define the cytosolic versus cortical staining of RhoA (Fig 3C). Quantification of the total cortical RhoA intensity displayed no significant difference in cells treated with control or Anx2 siRNA (Fig 3D, upper panel). However, in annexin A2-depleted cells, RhoA appeared to be localized all around the cell periphery and no more concentrated at the equator (Fig 3C), suggesting instead a polarization defect at the cortex. Measure of the ratio of the fluorescent intensity at the polar and equatorial cortical regions indeed indicates a 48% decrease in RhoA staining intensity in cells depleted for annexin A2 (Fig 3D). Annexin A2 thus seems to be necessary to restrict the zone of RhoA to the narrow cleavage furrow region and thus provides a mechanistic explanation for the early cytokinetic defect observed in annexin A2-depleted cells.

**Annexin A2 is required for the coupling of the central spindle to the equatorial cortex**

The activation of RhoA at the equatorial cortex depends on the centralspindlin which localizes in anaphase at central spindle midzone and thereby defines the position of the contractile ring assembly. The MgcRacGAP subunit of the centralspindlin directly binds and recruits the RhoA activator RhoGEF Ect2 to the midzone, which then translocates to the adjacent equatorial plasma membrane to activate RhoA [4–6,18,19]. We thus examined the localization of Ect2 and the two subunits of the centralspindlin MKLP1 and MgcRacGAP in annexin A2-depleted cells. While in control cells Ect2 is clearly detected at the cortex adjacent to the central spindle midzone, in annexin A2-depleted cells no Ect2 is visible at the equatorial cortex (Fig 4A, arrowhead and Fig 4B and C). However, both in control cells and in annexin A2-depleted cells, the two subunits of the centralspindlin are correctly recruited to the midzone of the central spindle (Fig 4A and D). Ect2 is also recruited to the spindle midzone, where it colocalizes with MgcRacGAP (Fig 4A), suggesting that neither the localization of centralspindlin nor the interaction between Ect2 and MgcRacGAP is affected in annexin A2-depleted cells. Furthermore, localization of the centralspindlin in MyrPalm-GFP cells to visualize the plasma membrane clearly shows that in the absence of annexin A2, MKLP1 and MgcRacGAP do not localize underlying the equatorial cortex and that the central spindle does not remain associated with the plasma membrane (Fig 4D). These results suggest that annexin A2 is necessary for the localization of Ect2 at the equatorial plasma membrane and for the maintenance of a connection between the central spindle and the cortex.

We describe here for the first time a role for annexin A2 in the progression through mitosis. The absence of rescue of the annexin A2 depletion phenotype by an annexin mutated for the S100A10 binding site (Figs 1C, 3E and 4C) indicates that the annexin A2-S100A10 heterodimer is implicated in the establishment of the cytokinetic furrow. Albeit the $AnxA2^{-/-}$ knockout mouse is viable, it is most likely that one of the 12 annexin vertebrate paralogs may compensate for annexin A2 function in the absence of the protein. One good candidate is the S100A6 binding annexin A11 which has been shown to play a role in the late phases of cytokinesis [20].

Our live cell imaging result shows that annexin A2 accumulates at the equatorial cortex. PIP2 have been shown to be an anchor for annexin A2 [21] and to regulate the recruitment of annexin A2 to the apical plasma membrane during epithelia cell polarization [13]. The cleavage furrow plasma membrane is enriched in $Ca^{2+}$ and PI(4,5)P2 which are key determinants required for setting and completion of cytokinesis [22]. Interaction with these lipids may thus contribute to the recruitment of annexin A2 at the cytokinetic furrow. Interestingly, growth factor-triggered phosphorylation of annexin A2 has previously been reported in interphasic cells to be necessary for Rho/Rock-dependent actin cytoskeleton remodeling [14,15].

Our data indicate that annexin A2 is required for the spatial restriction of RhoA localization at the equatorial plasma membrane. We cannot exclude that annexin A2 may play a role as a scaffold that directly recruits or stabilizes the polarized localization of RhoA. However, the exchange factor activity of Ect2 as well as its association with the plasma membrane has been shown to be required for the concentration of RhoA at the equatorial cortex [18]. The observation that in the absence of annexin A2, Ect2 is not detected at the plasma membrane while it is correctly recruited by MgcRacGAP at the central spindle suggests that annexin A2 functions upstream of RhoA. How Ect2 is recruited from the central spindle to the adjacent cortex is not well defined. Traffic between the central spindle and the cortex has been proposed to be actin dependent [23]. Annexin A2 regulates actin-dependent vesicular traffic. In epithelial cells, annexin A2 plays a role in the polarized delivery of specific cargos from the Rab11 vesicle to the PIP2-enriched apical plasma membrane [24,25]. Annexin A2 could be involved in the routing of RhoA and/or Ect2 to the PIP2-rich equatorial membrane domain.

Alternatively, annexin A2 may be necessary to maintain a close interaction between the central spindle and the plasma membrane and thereby favor the recruitment of Ect2 at the equatorial cortex. Even though various components of the central spindle such as MgcRacGAP can directly interact with PIP2 [26] or cortical elements [27], our observation that annexin A2 is required for the early steps of the formation of the cytokinetic furrow raises the possibility that annexin A2 may be involved in stabilization at the early steps of
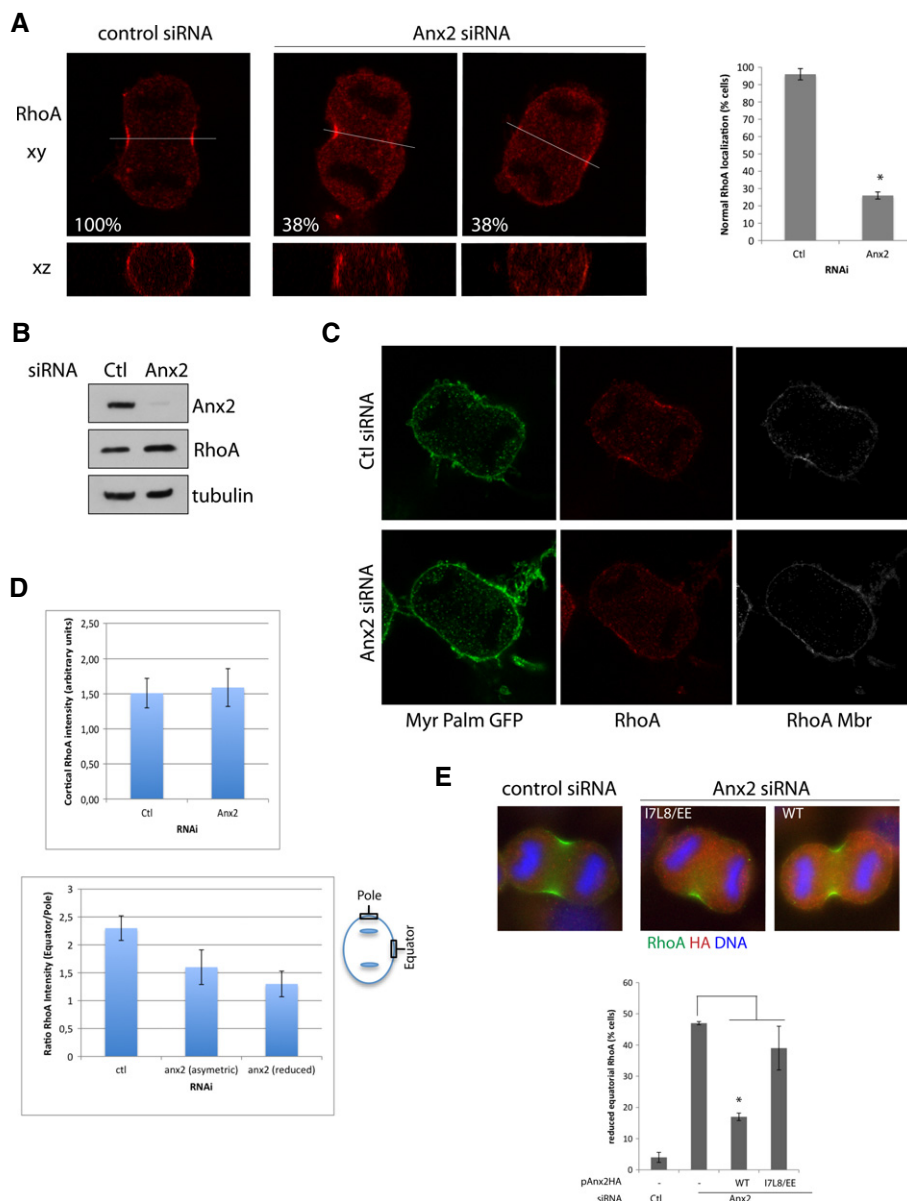
Figure 3.    Annexin A2 controls RhoA localization.

A    Confocal images of HeLa cells transfected with control or Anx2 RNAi and stained in anaphase with anti-RhoA antibody. *x–y* sections (top image) and *x–z* sections corresponding to the white line (bottom) are shown. Indicated percentages correspond to the ratio of cells in anaphase displaying the represented phenotype (*n* ≥ 50). Percentage of cells transfected with Ctl or Anx2 siRNA displaying normal equatorial cortex RhoA staining (graph). Error bars, SD of three experiments (*n* = 70). *P = 0.001, Student's *t*-test.

B    Immunoblotting of HeLa cells treated with control or Anx2 siRNA analyzed with anti-annexin A2, anti-tubulin and anti-RhoA antibodies.

C    HeLa cells stably expressing MyrPalm-GFP were transfected with Ctl RNAi or Anx2 RNAi and immunostained with anti-RhoA. Cortical RhoA staining (RhoA Mbr) corresponds to the RhoA staining defined by the MyrPalm-GFP mask.

D    Quantification of total cortical RhoA intensity in cells treated with control and Anx2 RNAi (top panel). Quantification of the accumulation of RhoA at the equatorial cortex expressed as the ratio of equatorial intensity over polar intensity (bottom panel). Error bars, SD of three experiments (*n* ≥ 20). Measured equatorial and polar regions are defined by the boxes on the diagram (bottom panel).

E    Immunofluorescence and quantification of RhoA localization in HeLa cells co-transfected with Ctl or Anx2 siRNA and pAnx2HA-WT or I7L8/EE mutant. Error bars, SD of three experiments (*n* ≥ 90). *P = 0.0001, Student's *t*-test.

recruitment prior to their accumulation at the equatorial cortex. Although we cannot exclude that the uncoupling of the central furrow and the equatorial cortex constriction observed in the absence of annexin A2 is only a downstream consequence of the alteration of RhoA function, a role for annexin A2 as a new molecular link between the central spindle and the contractile ring needs to be investigated now. Our results suggest that annexin A2 is required to transmit the spatial positioning of central spindle to the equatorial cortex. This study has thus indentified a new molecular interactor implicated in the formation of the actomyosin ring.
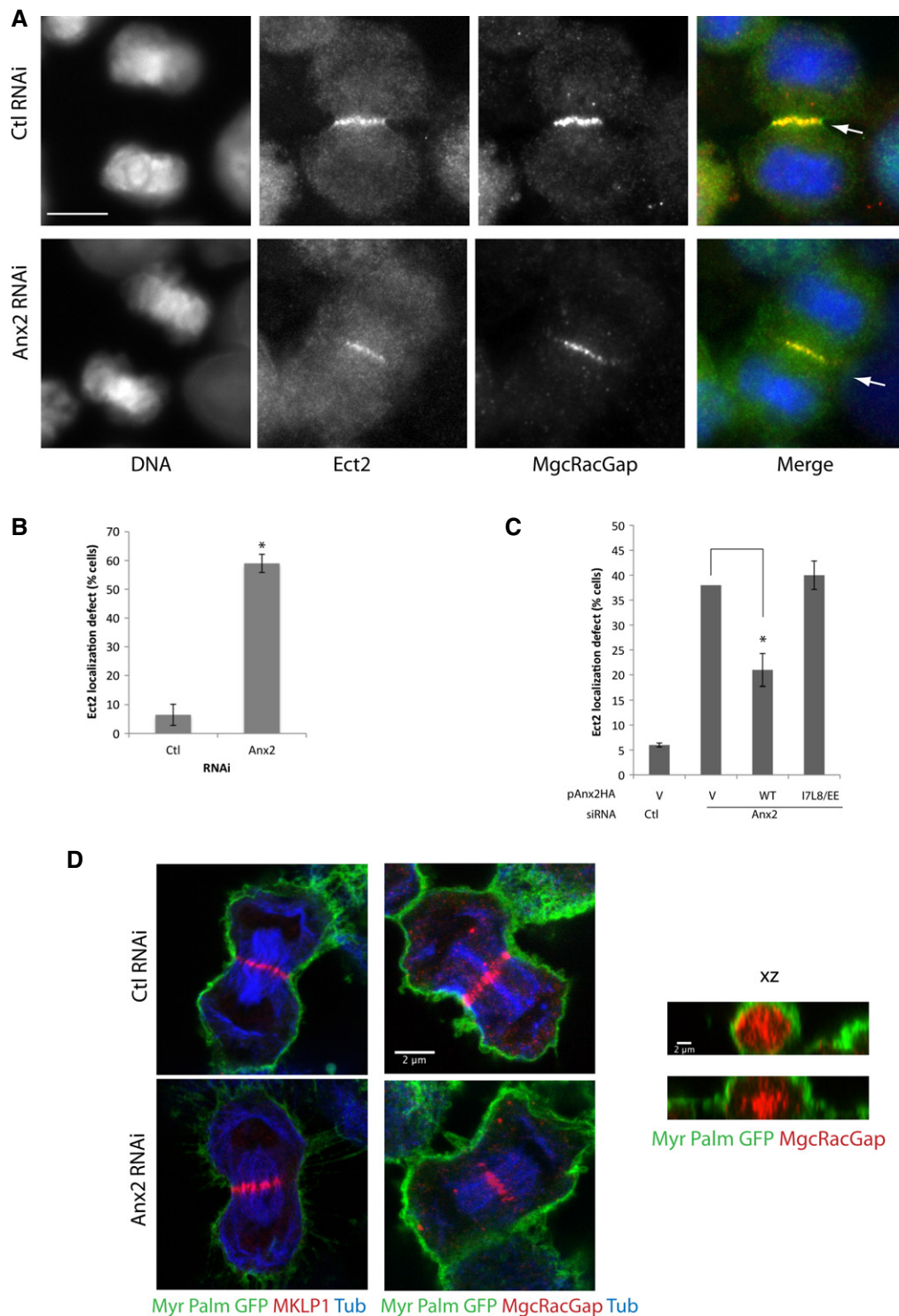
**Figure 4. Annexin A2 is required for cortical localization of Ect2 and plasma membrane association with the central spindle.**

A  Immunofluorescence images of HeLa cells transfected with control or annexin A2 RNAi, fixed in anaphase and co-labeled for DNA, Ect2 and MgcRacGAP. Arrows indicate the equatorial plasma membrane. Scale bar, 10 μm.

B  Quantification of the percentage of cells displaying cortical Ect2 localization in anaphase. Error bars, SD of four experiments ($n \geq 60$ each). *$P$ = 0.0002, Student's *t*-test.

C  Quantification of the percentage of cells with defective Ect2 localization in HeLa cells co-transfected with Ctl or Anx2 siRNA and pAnx2HA-WT or I7L8/EE mutant. Error bars, SD of three experiments ($n$ = 90). *$P$ = 0.005, Student's *t*-test.

D  Confocal images of MyrPalm-GFP-expressing HeLa cells transfected with control or annexin A2 RNAi. Cells were co-immunostained either for GFP/MKLP1/tubulin or for GFP/MgcRacGAP/tubulin. *x–y* sections (left panel) or *x–z* sections through the equatorial plane (right panel).

# Materials and Methods

### Cell culture and synchronization

HeLa Kyoto cells were grown in Dulbecco's modified Eagle's medium and Glutamax and U2OS cells in McCys's 5A medium (Gibco), both supplemented with 10% fetal calf serum (PAA), 100 U/ml penicillin and 100 μg/ml streptomycin. For synchronization experiments, cells were treated for 16 h with 5 μM RO-3306 (Merck), washed in complete medium and released for 40–60 min to reach anaphase.

### Expression constructs and stable cell lines

Human annexin A2 was cloned from a HeLa RT–PCR library and inserted with a HA tag using Topo cloning into pEntry plasmid and then recombined into pcDNA/V5-DEST (Invitrogen) or into pcDNA-DEST47 (annexin A2-GFP). Silent mutation for siRNA resistance against Anx2-1 siRNA (pAnx2HA WT and psiresAnnexinA2-GFP) was introduced using the Quick Change Lightning Multi Site-Directed Mutagenesis kit (Stratagene). I7L8/EE point mutations were then introduced to generate the annexin A2 S100A10 binding site mutant (pAnx2HA I7L8/EE) [28]. Stable cell line expressing annexin A2-GFP was generated by transfection of psiresAnnexinA2, and cells expressing the highest level of annexin A2-GFP were enriched by FACS sorting. About 90% of the stable annexin A2-GFP stable cell line population expressed the transgene. Since no stable cell line with a level of expression of the transgene close to the endogenous protein could be generated with the I7L8/EE mutant, only a transient rescue experiment was performed with the annexin A2 mutant.

pMyrPalm_mGFP and pLifeAct-mCherry (Addgene) were used to generate the MyrPalm-GFP and LifeAct HeLa stable cell lines, respectively.

### siRNA and plasmids transfection

A total amount of 25 nM of either control siRNA, Anx2-1 siRNA [29] or AnxA2-2, AnxA2-4, AnxA2-8 siRNAs (Qiagen) were transfected using Jetprime transfection reagents (Polyplus). Cells were analyzed either 36 h after transfection for anaphase analysis (immunofluorescence, video microscopy) or 48 h for multinucleation analysis. For transient rescue experiments, 15 nM siRNA and pAnx2HA WT or I7L8/EE were co-transfected.

### Antibodies, immunoblotting and immunofluorescence

The following commercial antibodies were used: annexin II, annexin II light chain (S100A10) (BD Transduction laboratory), tubulin clone YL1/2 and Ect2 (Millipore), HA.11 (Covance), myosin II and RacGAP1 (Abcam), phalloidin Alexa 568 (Life Technologies), anillin, RhoA and MKLP1 (Santa Cruz Biotechnology). Total cell lysis and immunoblotting were performed as described earlier [29]. For immunofluorescence, cells were grown on glass coverslips and fixed with either methanol at −20°C (tubulin, Ect2, RacGAP, MKLP1) or 4% paraformaldehyde in PBS (phalloidin) and 10% trichloroacetic acid (anillin, RhoA) at room temperature for 10 min, followed by 0.3% Triton for 10 min.

Antibody staining was then performed as described previously [29].

### Live cell imaging and microscopy

For live imaging, HeLa cells were grown in Lab-Tek I chambered cover glasses (Nunc) and transfected as described above. Bright field images of dividing cells were acquired every minute with a 25× objective on a DMRIBE inverted microscope (Leica) equipped with $CO_2$ heated incubator chamber and a CoolSNAP ES BW camera (Roper scientific). For bright field images with DNA staining of dividing cells, cells were synchronized and incubated with 0.02 μg/ml Hoechst 33342 as they were released. Images were acquired every minute with a 20×/0.85 NA objective on a LED-illuminated Deltavision equipped with a heated chamber and a CoolSnapHQ Princeton BW camera. Spinning confocal images were acquired using a Plan Apo 60×/1.4 NA objective on a Eclipse Ti-E microscope (Nikon) equipped with a spinning disk (CSU-X1; Yokogawa), a thermostatic chamber (Life Imaging Service), Z Piezo stage (Marzhauser) and a charge-coupled device camera (CoolSNAP HQ2; Roper Scientific). Time-lapse images were acquired every minute using the Metamorph Software (Universal imaging). Movies were constructed from image stacks saved in AVI 8fps under Fiji. Immunofluorescence images of fixed samples were acquired either with DMRXA2 epifluorescence microscope or with SP5 confocal microscope (Leica). Images were processed and quantified using Fiji software (http://fiji.sc/). Student's *t*-test was used for statistical analysis.

## Author contributions
CB designed and performed the experiments. The molecular biology was carried out by GLD. SM and FG performed the experiments. DR participated in the design of experiments and the discussion of the results and manuscript. CP provided input on the project. The manuscript was written by CB.

## Conflict of interest
The authors declare that they have no conflict of interest.

# References

1. Fededa JP, Gerlich DW (2012) Molecular control of animal cell cytokinesis. *Nat Cell Biol* 14: 440–447

2. Watanabe S, Ando Y, Yasuda S, Hosoya H, Watanabe N, Ishizaki T, Narumiya S (2008) mDia2 induces the actin scaffold for the contractile ring and stabilizes its position during cytokinesis in NIH 3T3 cells. *Mol Biol Cell* 19: 2328–2338

3. Matsumura F (2005) Regulation of myosin II during cytokinesis in higher eukaryotes. *Trends Cell Biol* 15: 371–377

4.   Nishimura Y, Yonemura S (2006) Centralspindlin regulates ECT2 and RhoA accumulation at the equatorial cortex during cytokinesis. *J Cell Sci* 119: 104−114

5.   Yüce Ö, Piekny A, Glotzer M (2005) An ECT2-centralspindlin complex regulates the localization and function of RhoA. *J Cell Biol* 170: 571−582

6.   Chalamalasetty RB, Hummer S, Nigg EA, Sillje HH (2006) Influence of human Ect2 depletion and overexpression on cleavage furrow formation and abscission. *J Cell Sci* 119: 3008−3019

7.   Grieve AG, Moss SE, Hayes MJ (2012) Annexin A2 at the interface of actin and membrane dynamics: a focus on its roles in endocytosis and cell polarization. *Int J Cell Biol* 2012: 852430

8.   Gerke VCC, Creutz CE, Moss SE (2005) Annexins: linking Ca$^{2+}$ signalling to membrane dynamics. *Nat Rev Mol Cell Biol* 6: 449−461

9.   Morel E, Parton RG, Gruenberg J (2009) Annexin A2-dependent polymerization of actin mediates endosome biogenesis. *Dev Cell* 16: 445−457

10.  Hayes MJ, Merrifield CJ, Shao D, Ayala-Sanmartin J, Schorey CD, Levine TP, Proust J, Curran J, Bailly M, Moss SE (2004) Annexin 2 binding to phosphatidylinositol 4,5-bisphosphate on endocytic vesicles is regulated by the stress response pathway. *J Biol Chem* 279: 14157−14164

11.  Merrifield CJ, Rescher U, Almers W, Proust J, Gerke V, Sechi AS, Moss SE (2001) Annexin 2 has an essential role in actin-based macropinocytic rocketing. *Curr Biol* 11: 1136−1141

12.  Zobiack N, Rescher U, Laarmann S, Michgehl S, Schmidt MA, Gerke V (2002) Cell-surface attachment of pedestal-forming enteropathogenic *E. coli* induces a clustering of raft components and a recruitment of annexin 2. *J Cell Sci* 115: 91−98

13.  Martin-Belmonte F, Gassama A, Datta A, Yu W, Rescher U, Gerke V, Mostov K (2007) PTEN-mediated apical segregation of phosphoinositides controls epithelial morphogenesis through Cdc42. *Cell* 128: 383−397

14.  Babbin BA, Parkos CA, Mandell KJ, Winfree LM, Laur O, Ivanov AI, Nusrat A (2007) Annexin 2 regulates intestinal epithelial cell spreading and wound closure through rho-related signaling. *Am J Pathol* 170: 951−966

15.  Rescher U, Ludwig C, Konietzko V, Kharitonenkov A, Gerke V (2008) Tyrosine phosphorylation of annexin A2 regulates Rho-mediated actin rearrangement and cell adhesion. *J Cell Sci* 121: 2177−2185

16.  Sauer G, Körner R, Hanisch A, Ries A, Nigg EA, Silljé HHW (2005) Proteome analysis of the human mitotic spindle. *Mol Cell Proteomics* 4: 35−43

17.  Piekny AJ, Glotzer M (2008) Anillin is a scaffold protein that links RhoA, actin, and myosin during cytokinesis. *Curr Biol* 18: 30−36

18.  Su K-C, Takaki T, Petronczki M (2011) Targeting of the RhoGEF Ect2 to the equatorial membrane controls cleavage furrow formation during cytokinesis. *Dev Cell* 21: 1104−1115

19.  Petronczki M, Glotzer M, Kraut N, Peters JM (2007) Polo-like kinase 1 triggers the initiation of cytokinesis in human cells by promoting recruitment of the RhoGEF Ect2 to the central spindle. *Dev Cell* 12: 713−725

20.  Tomas A, Futter C, Moss SE (2004) Annexin 11 is required for midbody formation and completion of the terminal phase of cytokinesis. *J Cell Biol* 165: 813−822

21.  Rescher U, Ruhe D, Ludwig C, Zobiack N, Gerke V (2004) Annexin 2 is a phosphatidylinositol (4,5)-bisphosphate binding protein recruited to actin assembly sites at cellular membranes. *J Cell Sci* 117: 3473−3480

22.  Janetopoulos C, Devreotes P (2006) Phosphoinositide signaling plays a key role in cytokinesis. *J Cell Biol* 174: 485−490

23.  Hu C-K, Coughlin M, Field CM, Mitchison TJ (2008) Cell polarization during monopolar cytokinesis. *J Cell Biol* 181: 195−202

24.  Bryant DM, Datta A, Rodriguez-Fraticelli AE, Peranen J, Martin-Belmonte F, Mostov KE (2010) A molecular network for *de novo* generation of the apical surface and lumen. *Nat Cell Biol* 12: 1035−1045

25.  Jacob R, Heine M, Eikemeyer J, Frerker N, Zimmer K-P, Rescher U, Gerke V, Naim HY (2004) Annexin II is required for apical transport in polarized epithelial cells. *J Biol Chem* 279: 3680−3684

26.  Lekomtsev S, Su KC, Pye VE, Blight K, Sundaramoorthy S, Takaki T, Collinson LM, Cherepanov P, Divecha N, Petronczki M (2012) Centralspindlin links the mitotic spindle to the plasma membrane during cytokinesis. *Nature* 492: 276−279

27.  D'Avino PP, Takeda T, Capalbo L, Zhang W, Lilley KS, Laue ED, Glover DM (2008) Interaction between Anillin and RacGAP50C connects the actomyosin contractile ring with spindle microtubules at the cell division site. *J Cell Sci* 121: 1151−1158

28.  Thiel C, Osborn M, Gerke V (1992) The tight association of the tyrosine kinase substrate annexin II with the submembranous cytoskeleton depends on intact p11- and Ca$^{2+}$-binding sites. *J Cell Sci* 103(Pt 3): 733−742

29.  Benaud C, Gentil BJ, Assard N, Court M, Garin J, Delphin C, Baudier J (2004) AHNAK interaction with the annexin 2/S100A10 complex regulates cell membrane cytoarchitecture. *J Cell Biol* 164: 133−144